*J Biosci* (2019) 44:86
DOI: 10.1007/s12038-019-9895-1


# Adiponectin inhibits vascular smooth muscle cell calcification induced by beta-glycerophosphate through JAK2/STAT3 signaling pathway

Yan Lu[1], Yichao Ma[1], Ruihua Wang[1], Jing Sun[1], Beibei Guo[1], Ruipeng Wei[1] and Yongping Jia[2]*

[1]*Department of Cardiology, The First Hospital of Shanxi Medical University, No. 85 Jiefangnan Road, Taiyuan 030001, Shanxi, People's Republic of China*

[2]*Shanxi Medical University, No. 56 Xinjiannan Road, Taiyuan 030001, Shanxi, People's Republic of China*

**Corresponding author (Email, jiayp914@163.com)*

*MS received 18 December 2018; accepted 29 April 2019; published online 5 August 2019*

Vascular calcification is a common problem in the elderly with diabetes, heart failure and end-stage renal disease. The differentiation of vascular smooth muscle cells (VSMCs) into osteoblasts is the main feature, but the exact mechanism remains unclear. It is not clear whether adiponectin (APN) affects osteogenic differentiation of VSMCs. This study aims to explore the effect of APN on vascular calcification by using a cell model induced by beta-glycerophosphate (β-GP). VSMCs were isolated and treated with β-GP and APN in this study. The alkaline phosphatase (ALP) activity and expression levels of Runx2, BMP-2, collagen type I and osteocalcin were determined. The expression levels of STAT3 and p-STAT3 in nucleus and cytoplasm of VSMCs were analyzed. The results showed that APN significantly inhibited the expression of ALP, Runx2, BMP-2, collagen I, osteocalcin and the formation of the mineralized matrix in VSMCs induced by β-GP. APN reduces the osteogenic differentiation of VSMCs induced by β-GP and down-regulates the expression of the osteogenic transcription factor osterix by inhibiting STATS3 phosphorylation and nuclear transport. APN may be one of the potential candidates for clinical treatment of vascular calcification.

**Keywords.** Adiponectin; JAK2/STAT3; vascular calcification; vascular smooth muscle

## 1. Introduction

Vascular calcification is a common problem in the elderly with diabetes, heart failure and end-stage renal disease. It is associated with myocardial infarction, impaired vascular tension and poor prognosis after angiogenic surgery (Chen and Moe 2015; Nitta and Ogawa 2015; Cardenas *et al.* 2018; Chen *et al.* 2018; Cheng *et al.* 2018; Jasani *et al.* 2018). Recent studies found that the calcification process of vascular smooth muscle cells (VSMCs) is basically consistent with bone formation. This process involves the expression of osteoblast-like markers of VSMCs and the formation of bone hydroxyapatite and matrix vesicles in cells (Leopold 2015). The exact mechanism of vascular calcification is unclear. To explore the mechanism of osteoblast differentiation in VSMCs will help to further understand vascular calcification and to formulate effective strategies for the treatment of vascular calcification.

Adiponectin (APN) is a circulating cytokine secreted by adipocytes, it contains 22 collagen repeat handles and a highly conserved globular domain (GAD). There are three main forms of APN in human and mouse, including trimer, hexamer and high-molecular weight form. GAD is a functional form of APN. It is reported that GAD has higher bioactivity than the full-length form (Pajvani *et al.* 2003). APN has a significant regulatory effect on metabolism, it has protective effects on metabolic syndrome, liver fibrosis, canceration and myocardial IRI (Sun *et al.* 2011; Moon and Mantzoros 2013; Ding *et al.* 2016; Li *et al.* 2016; Wang *et al.* 2016). It was found that APN was closely related to cardiovascular disease. Plasma APN levels were significantly decreased in hypertensive patients, and hypoadiponectinemia was an independent risk factor for essential hypertension (Guo *et al.* 2018). APN can inhibit the proliferation of VSMCs by reducing the synthesis of cell DNA mediated by platelet-derived growth factors and fibroblast cytokines (Uemura *et al.* 2013). APN can also induce the activation of eNOS in VSMCs, thereby upregulate the production of NO, which is conducive to vasodilatation (Zhang *et al.* 2013). APN is a marker of endothelial dysfunction in APN knockout mice (Liu *et al.* 2015). At the same time,

APN can also play an anti-atherosclerosis role by inhibiting the over-activation of the NF-kB signaling pathway and the expression of adhesion molecules in vascular endothelial cells, and reducing the local adhesion of monocytes (Zhang *et al.* 2014). As far as we know, whether APN plays a role in the process of vascular calcification has not been reported.

JAK-mediated signaling pathways are associated with surface receptors of many cytokines and play an important role in bone development and metabolism. JAK kinase 2 (JAK2)/signal transduction and activator transcription 3 (STAT3) is an intracellular signal transduction pathway that has been reported to be associated with a variety of cardiovascular diseases. Vascular calcification is characterized by inflammation and differentiation of vascular endothelial cells into osteoblasts. Therefore, cytokine-mediated activation of the JAK2/STAT3 signaling pathway may be essential for osteogenic differentiation and calcification of vascular endothelial cells. Inhibition of the JAK2/STAT3 signaling pathway may improve vascular calcification. In this study, we explored the molecular mechanism of APN inhibiting VSMC calcification through the JAK2/STAT3 signaling pathway.

## 2. Methods

### 2.1 *Experimental animals*

C57BL/6 mice (4–6 week old, weight 16–20 g) were purchased from Shanghai SLAC Laboratory Animal CO. Ltd. They were bred in the SPF class barrier system of the Anhui experimental animal center, and were allowed to eat and drink freely. All experiments on animals were conducted according to Principles of Laboratory Animal Care (National Society for Medical Research).

This study was approved by the ethical committee of the first hospital of Shanxi Medical University. All experiments were conducted according to the principles stated in the Declaration of Helsinki.

### 2.2 *Cell isolation and culture*

The mice were executed and soaked in 75% alcohol for 15 min. Pulmonary aorta vessels were taken out under sterile conditions, they were washed in PBS and gently scraped the outer membrane and intima tissues. They were cut into 1 mm × 1 mm tissue block and cultured with HG DMEM medium containing 20% fetal bovine serum (FBS) at 37°C with 5% $CO_2$. The medium was changed once every 3 d and they were cultured for about 15 d. The cells were passaged and cultured with HG DMEM medium containing 10% FBS at 37°C with 5% $CO_2$.

To determine the optimal concentration of APN, we treated VSMCs continuously with 0, 12.5, 25, 50, 100 and 200 μM APN for 48 h, respectively. Apoptosis was detected by using an Annexin V-FITC/PI apoptosis detection kit. The highest concentration without obvious apoptosis was 50 μM, which was used as the highest concentration of APN in subsequent experiments.

### 2.3 *Molecular mechanism analysis of alkaline phosphatase (APN) inhibiting VSMC calcification*

To observe the dose effect of APN on VSMC calcification, VSMCs were treated with 10 μM β-GP and with 0, 12.5, 25 and 50 μM APN for 7 d. The ALP activity and expression levels of Runx2, BMP-2, collagen type I and osteocalcin were determined.

To observe the time effect of APN on reducing calcification of VSMCs, VSMCs were treated with 10 μM β-GP and 50 μM APN for 3, 6, 9 and 12 d, the ALP activity, the expression levels of Runx2, BMP-2, collagen type I and osteocalcin were detected.

To analyze the mineralized matrix in cells, we treated VSMCs with 10 μM β-GP and 50 μM APN for 18 days. The cells were collected and stained with Alizarin red S.

The expression levels of STAT3 and p-STAT3 in nucleus and cytoplasm of VSMCs were analyzed after they were treated with 10 μM β-GP and 50 μM APN for 48 h. After VSMCs were treated with 10 μM β-GP, 50 μM APN and 50 μM AG490 for 48 h, the ALP activity and the expression levels of Runx2, BMP-2 and Osterix were detected.

To analyze the molecular mechanism of the JAK2/STAT3 signaling pathway involved in APN inhibiting VSMC calcification, the VSMCs were treated with 10 μM β-GP and transfected with STAT3 interfering plasmid shSTAT3 (Santa Cruz, Dallas, USA; sc-29494-SH) for 48 h, at the same time, the cells were treated with 50 μM APN and 50 μM AG490 for 48 h, respectively. Then the cells were collected and the ALP activity, Runx2, BMP-2 and osterix expression levels were analyzed.

### 2.4 *ALP activity determination*

The cells were harvested at different time points to detect ALP activity by the ALP activity detection kit (Beyotime, Shanghai, China). The cells were lysed with cell lysis solution (400 μL, Sigma-Aldrich, St. Louis, MO, USA) and incubated at 30°C for 4 h, and then the cells were collected and incubated for 30 min, they were detected using *p*-nitrophenyl disodium phosphate as the substrate. ALP activity in each group was calculated according to the standard. At the same time, the Bio-Rad protein assay kit (Bio-Rad, USA) was used to detect the total protein content of the cells according to the manual. ALP activity was expressed by pNP (mM)/total protein (mg).

### 2.5 *Ribonucleic acid (RNA) extraction and quantitative real-time polymerase chain reaction (qRT-PCR)*

Total RNA was extracted using a Trizol reagent kit (Invitrogen, Carlsbad, CA, USA) according to the manufacturer's protocol. RNA concentration and purity were detected using a NanoDrop™ 1000 Spectrophotometer (Thermo Fisher

**Table 1.** Primers used in this study

| Gene | Forward primer | Reverse primer |
|---|---|---|
| ALP | GACGGTGAACGGGAGAAC | GAACAGAGCCAGTGGAAGC |
| Runx2 | GACTGTGGTTACCGTCATGGC | ACTTGGTTTTTCATAACAGCGGA |
| Collagen I | TGACCAGCCTCGCTCACA | CGGGCAGGGTTCTTTCTA |
| BMP-2 | GGGACCCGCTGTCTTCTAGT | TCAACTCAAATTCGCTGAGGAC |
| Osterix | GGGGAAAGGAGGCACAAA | GGAGCAAAGTCAGATGGGTAA |
| Osteocalcin | ACTTGTGCTGGGTGGTCT | CAATACGCAGTGGCATTAA |
| β-Actin | TGAGGATGTCACGGTTCCAG | GTCACCTTCACCGTTCCAGT |

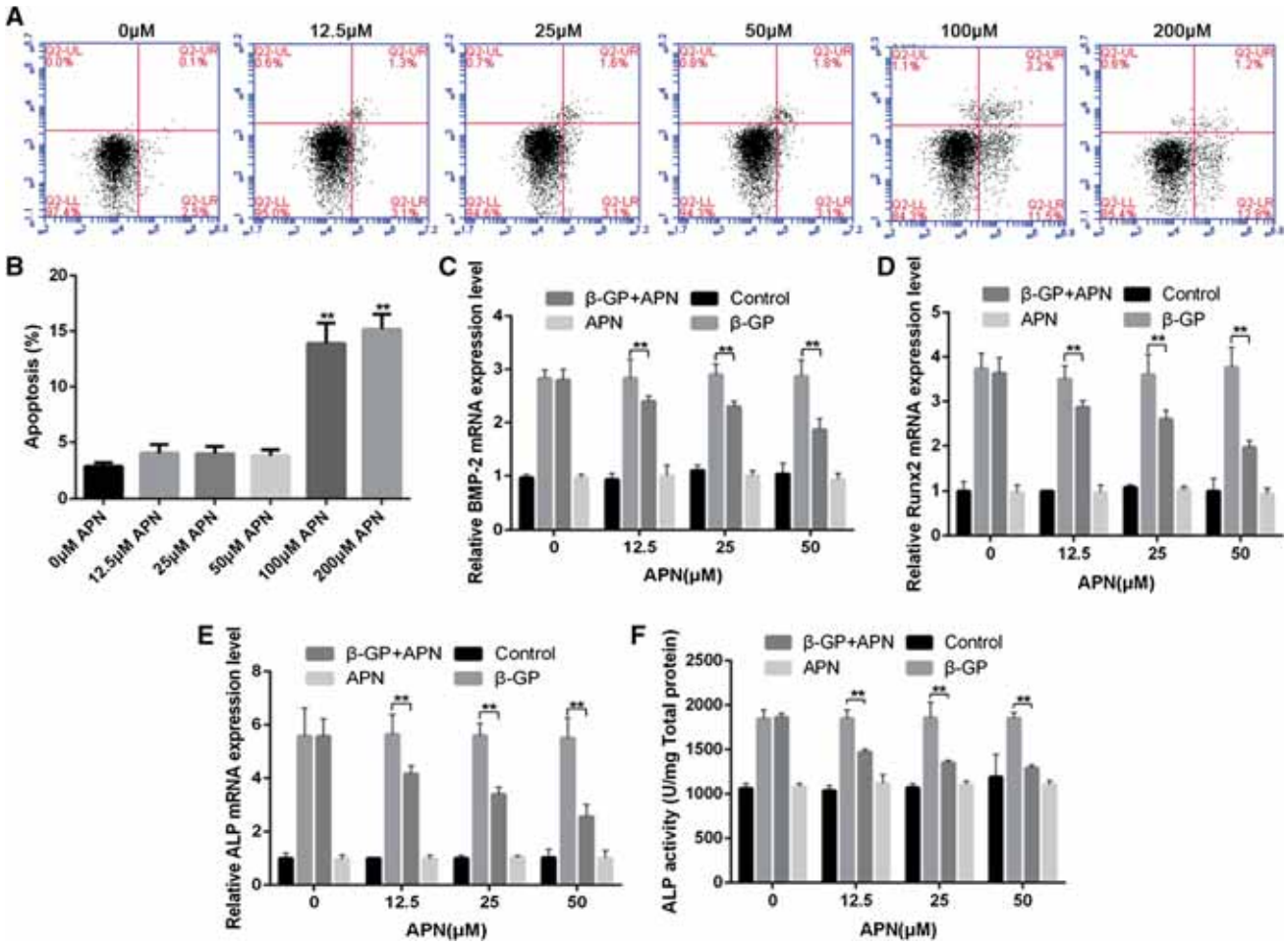


**Figure 1.** Effects of different doses of APN on ALP activity, RUNX2 and BMP-2 expression in VSMCs induced by β-GP. (**A**) VSMC apoptosis after the treatment of different doses of APN for 48 h; (**B**) the proportion of VSMC apoptosis in different groups; (**C**) BMP-2 mRNA expression in VSMCs induced by β-GP after they were treated with different doses of APN for 7 d; (**D**) Runx2 mRNA expression in VSMCs induced by β-GP after they were treated with different doses of APN for 7 d; (**E**) ALP mRNA expression in VSMCs induced by β-GP after they were treated with different doses of APN for 7 d and (**F**) ALP activity in VSMCs induced by β-GP after they were treated with different doses of APN for 7 d. $^{**}P < 0.01$ *vs* control.

Scientific, Inc.). A total of 1 μg RNA was subjected to reverse transcription using a RevertAid First Strand cDNA Synthesis Kit (Fermentas). qPCR was performed using a Maxima SYBR Green/Rox qPCR Master Mix (Fermentas) on the ABI StepOne Plus system (Applied Biosystems, Waltham, MA). The quantification method used was the $2^{-\Delta\Delta CT}$ method. The thermocycling conditions are as follows: Pre-degeneration at 95°C for 10 min, followed by 40 cycles of 95°C for 5 s and 60°C for 40 s; GAPDH gene was used as an internal control. The primers used in this study are shown in table 1.

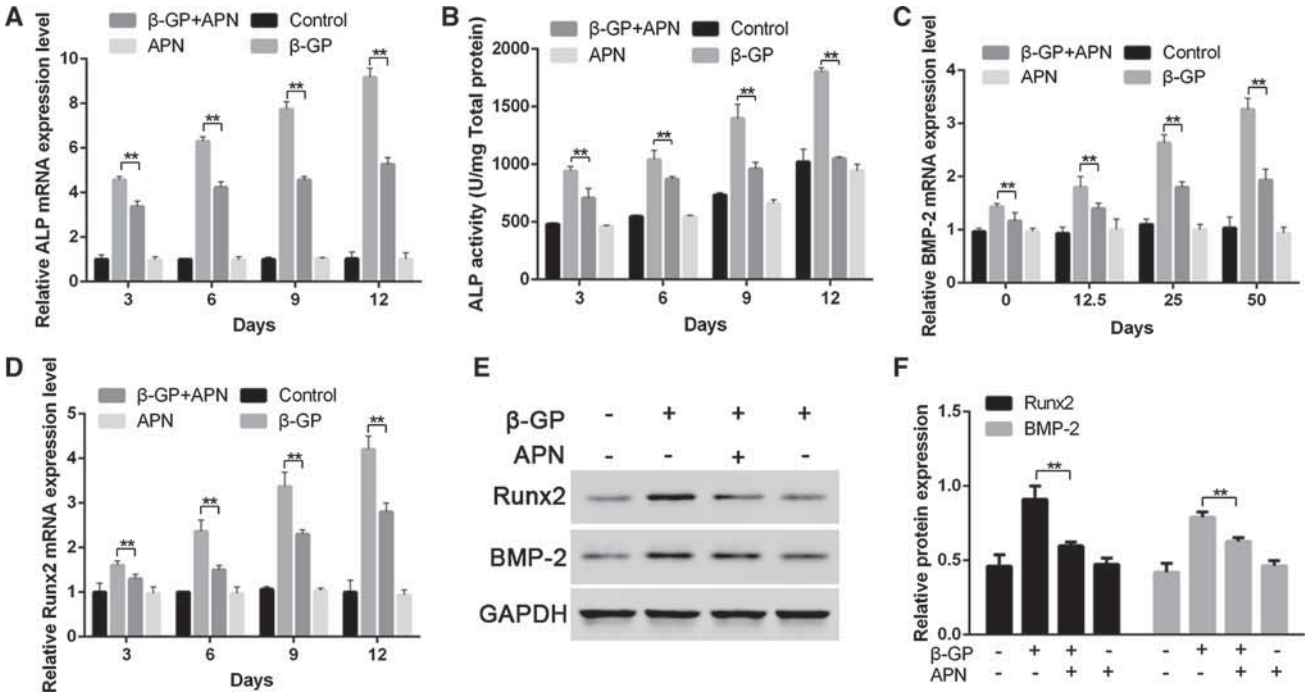


**Figure 2.** Effects of different time points of APN treatment on ALP activity, RUNX2 and BMP-2 expression in VSMCs induced by β-GP. (**A**) ALP mRNA expression changes in VSMCs induced by β-GP at different time points after they were treated with APN; (**B**) ALP activity changes in VSMCs induced by β-GP at different time points after they were treated with APN; (**C**) BMP-2 mRNA expression changes in VSMCs induced by β-GP at different time points after they were treated with APN; (**D**) Runx2 mRNA expression changes in VSMCs induced by β-GP at different time points after they were treated with APN; (**E**) RUNX2 and BMP-2 protein expression changes in VSMCs induced by β-GP at different time points after they were treated with APN and (**F**) gray value analysis of RUNX2 and BMP-2 protein relative expression levels. $^{**}P < 0.01$ *vs* control.

### 2.6 *Western blotting method*

Cells in the logarithmic growth period were harvested and the nuclear and cytoplasmic proteins are extracted using a Nuclear and Cytoplasmic Protein Extraction Kit (Beyotime, Shanghai, China) according to instructions. The protein concentration was determined using a BCA kit (Beyotime, Shanghai, China) according to instructions. Proteins (50 μg/lane) were separated using 12% SDS–PAGE. Proteins were then electrotransferred to a PVDF membrane (Amersham Biosciences, Piscataway, NJ, USA). The PVDF membrane was rinsed with TBS for 10–15 min, placed in TBS/T blocking buffer containing 5% (w/v) skimmed milk powder. It was incubated at room temperature for 2 h following the addition of an appropriate dilution of primary antibodies (1:1000 JAK2, Abcam, Cambridge, UK, ab205223; 1:2000 p-JAK2, Abcam, Cambridge, UK, ab32101; 1:2000 STAT3, Abcam, Cambridge, UK, ab68153; 1:1000 p-STAT3, Abcam, Cambridge, UK, ab76315; 1:500 osterix, 1:2000 Abcam, Cambridge, UK; ab209484; β-actin, Abcam, Cambridge, UK, ab8226). The membrane was then rinsed with TBST three times (5–10 min/wash) and then incubated at room temperature for 1 h with horseradish peroxidase-labeled secondary antibody (1:50,000; Abcam, Cambridge, UK; diluted with TBST containing 0.05% (w/v) skimmed milk powder). The membrane was then rinsed three times with Tris-Hcl+Tween20 buffer (TBST; 5–10 min/wash). Protein bands were detected using an enhanced chemiluminescence kit (Perkin-Elmer Inc.) and quantified as the ratio to β-actin. Quantification was performed using Imagequant LAS4000 (GE Healthcare, Japan).

### 2.7 *Measurement of mineralization matrix formation*

The cell crawling slides of different groups were fixed at room temperature with ethanol for 30 min. They were washed with 2 mL distilled water three times, and dyed with 1% Alizarin red S at 37°C for 1 h. Then they were washed with distilled water three times, the mineralized nodules in the cells were observed under a microscope (Zeiss, Jena, Germany) and images were taken. The proportion of positive areas was calculated using Image J (version 6.0, Media Cybernetics, Bethesda, MD) by selecting five horizons randomly.

### 2.8 *Cell apoptosis detected by flow cytometry assay*

Apoptosis analysis was performed by the AnnexinV-FITC Analysis Kit (Beyotime, Shanghai, China) according to the manual. Cells in each group were collected, digested with trypsin without ethylenediaminetetraacetic acid, and washed twice with ice-cold PBS. Collected $1 \times 10^6$ cells/mL by centrifugation and resuspended cells in 400 μL 1× binding

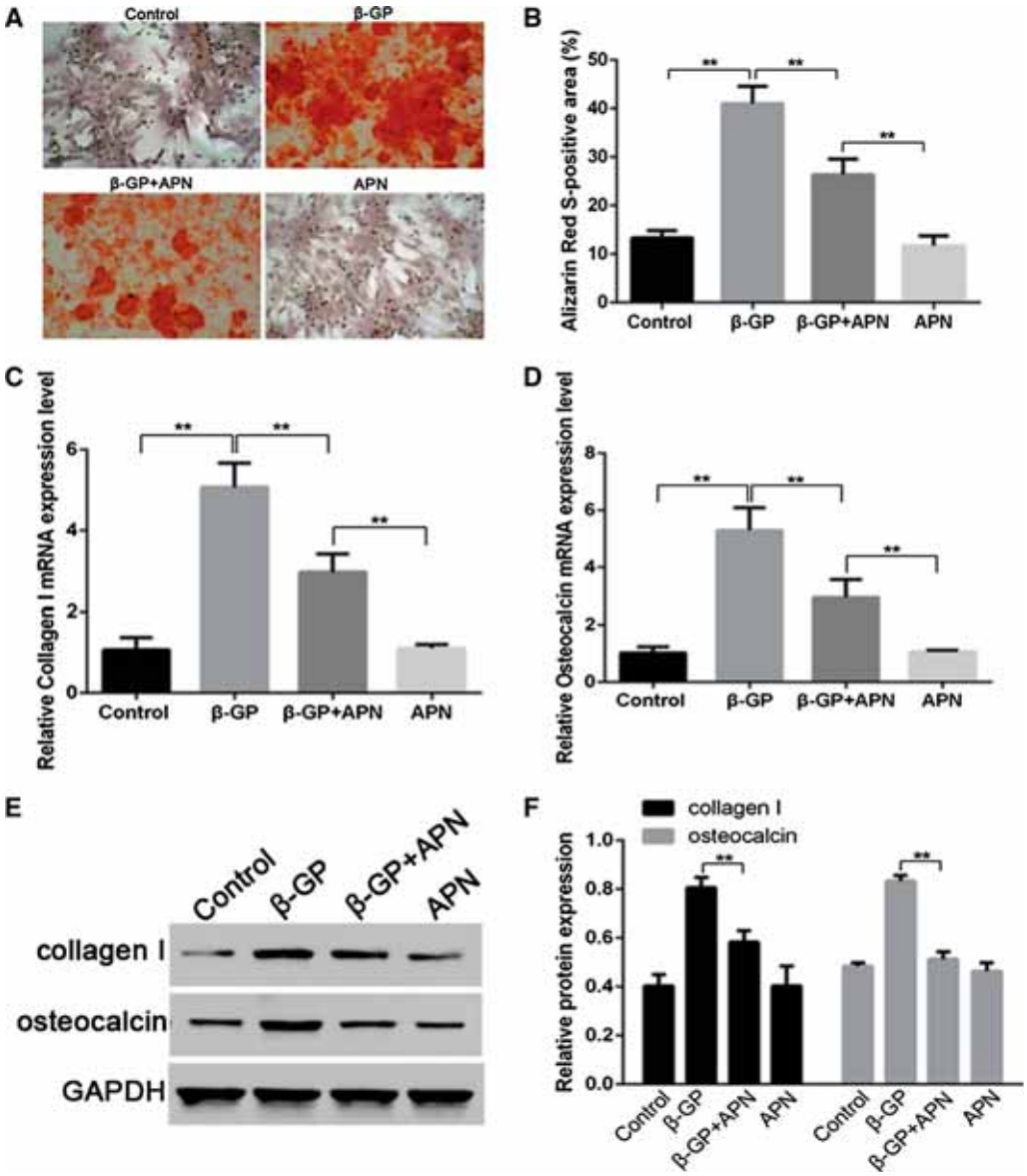


**Figure 3.** Effects of APN treatment on the formation of the mineralized matrix and the expression of collagen type I and osteocalcin in VSMCs induced by β-GP. (**A** and **B**) Alizarin red staining showed that APN could inhibit the formation of the mineralized matrix in VSMCs induced by β-GP; (**C** and **D**) qRT-PCR results showed that APN could inhibit the mRNA expression of collagen type I and osteocalcin in VSMCs induced by β-GP and (**E** and **F**) western blotting results showed that APN could inhibit the protein expression of collagen type I and osteocalcin in VSMCs induced by β-GP. $^{**}P < 0.01$ *vs* control.

buffer. Add 5 μL Annexin V-FITC (Beyotime, Shanghai, China) according to the manufacturer's protocol. After 15 min of incubation at a 4°C refrigerator in the dark, propidium iodide was added, and then incubated in a 4°C refrigerator for 5 min. The apoptosis rate was detected using flow cytometry (FACScan; BD Biosciences, San Jose, CA, USA), and the experiment was repeated thrice.

### 2.9 *Statistical analysis*

The data were analyzed using GraphPad Prism 6.0 (GraphPad Software Inc., La Jolla, CA, USA). All results are presented as the mean ± standard deviation. Student's *t* test and one-way ANOVA test were used to evaluate the differences among groups. $P < 0.05$ was considered to indicate a statistically significant difference.

## 3. Results

### 3.1 *APN could inhibit the osteogenic differentiation of VSMCs induced by β-GP*

The results of flow cytometry showed that it did not cause VSMC apoptosis when APN concentration was less than 50

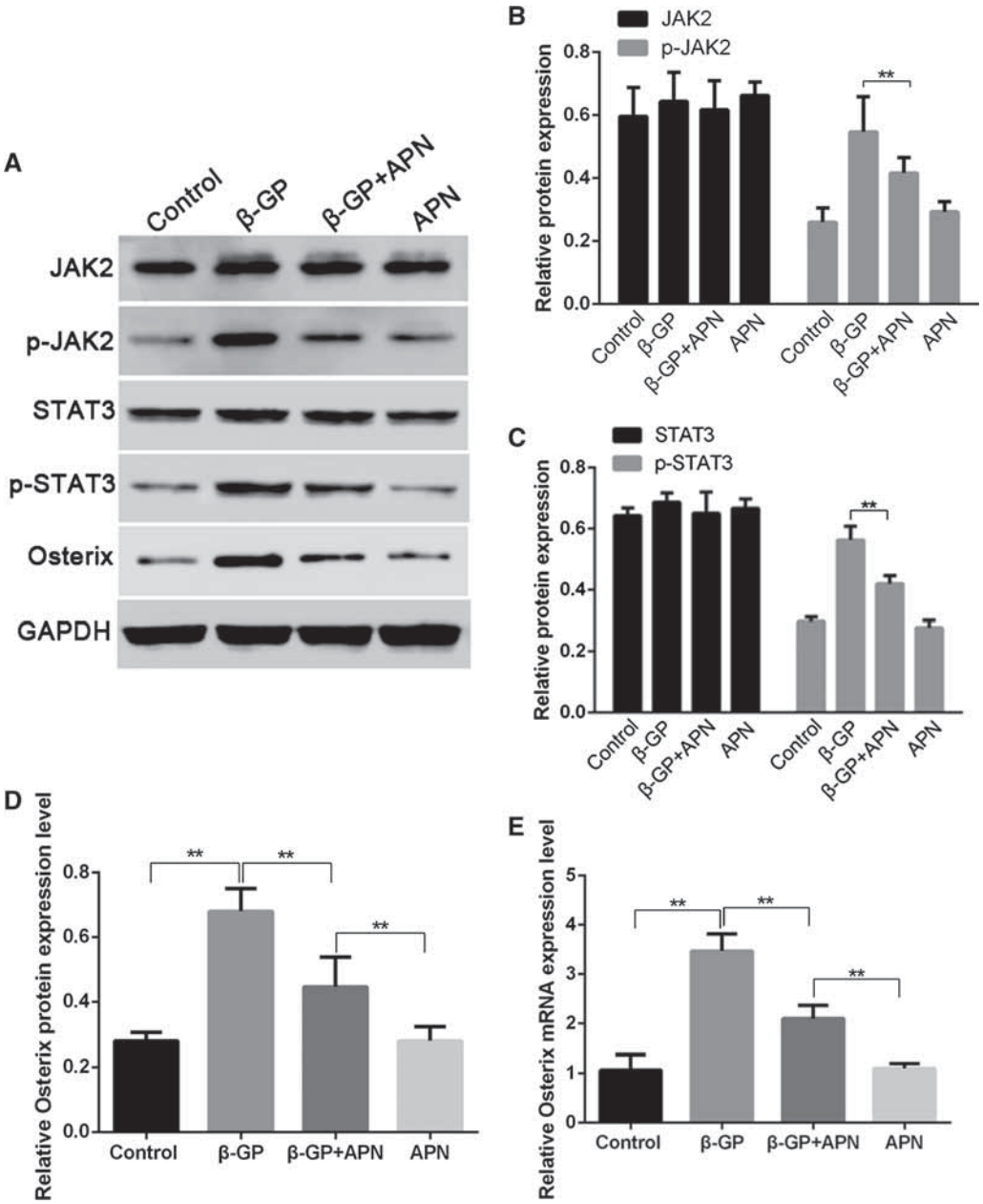


**Figure 4.** APN could inhibit the phosphorylation of STAT3 and down regulate the expression of osterix in VSMCs treated with β-GP. (**A**) Western blotting results of JAK2, p-JAK2, STAT3, p-STAT3 and osterix expression; (**B**) relative expression of JAK2 and p-JAK2; (**C**) relative expression of STAT3 and p-STAT3; (**D**) relative expression of osterix protein and (**E**) relative osterix mRNA expression. $^{**}P < 0.01$ *vs* control.

μM and treated for 48 h (figure 1A and B). The expression levels of ALP, Runx2 and BMP-2 are the indicators of VSMC calcification. The expression levels of ALP, Runx2 and BMP-2 mRNA were significantly inhibited with a dose-dependent manner when VSMCs induced by β-GP were treated with 12.5–50 μM APN (figure 1C–F).

The expression levels of ALP, Runx2 and BMP-2 decreased gradually with an increase of treatment time when VSMCs induced by β-GP were treated with 50 μM APN (figure 2).

The formation of the mineralized matrix and the expression of collagen type I and osteocalcin in VSMCs were significantly inhibited when VSMCs induced by β-GP were treated with 50 μM APN (figure 3).

### 3.2 *APN could inhibit the phosphorylation of STAT3 and transport into the nucleus, and down regulate the expression of osterix*

The JAK2/STAT3 signaling pathway participates in the bone formation regulation by regulating osteoblast differentiation and expression of osterix, a bone formation-related

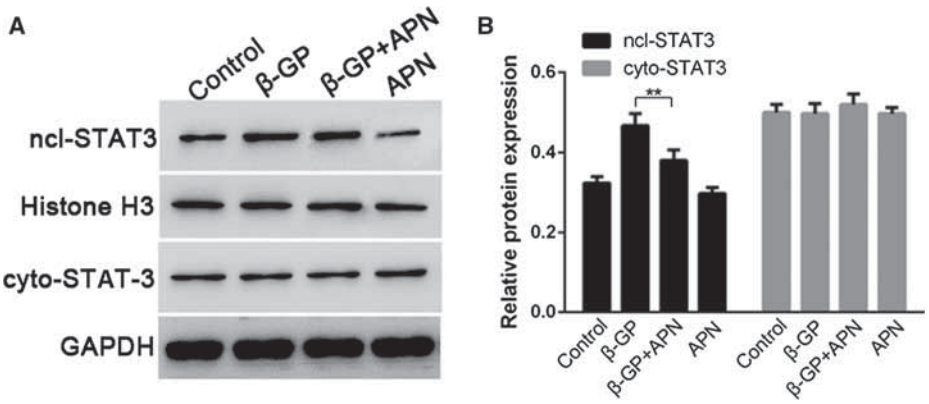


**Figure 5.** APN could inhibit STAT3 transport into the nucleus in VSMCs treated with β-GP. (**A**) Western blotting results of APN effects on nuclear transport of STAT3 in VSMCs treated with β-GP and (**B**) relative expression of STAT3. $^{**}P < 0.01$ *vs* control.

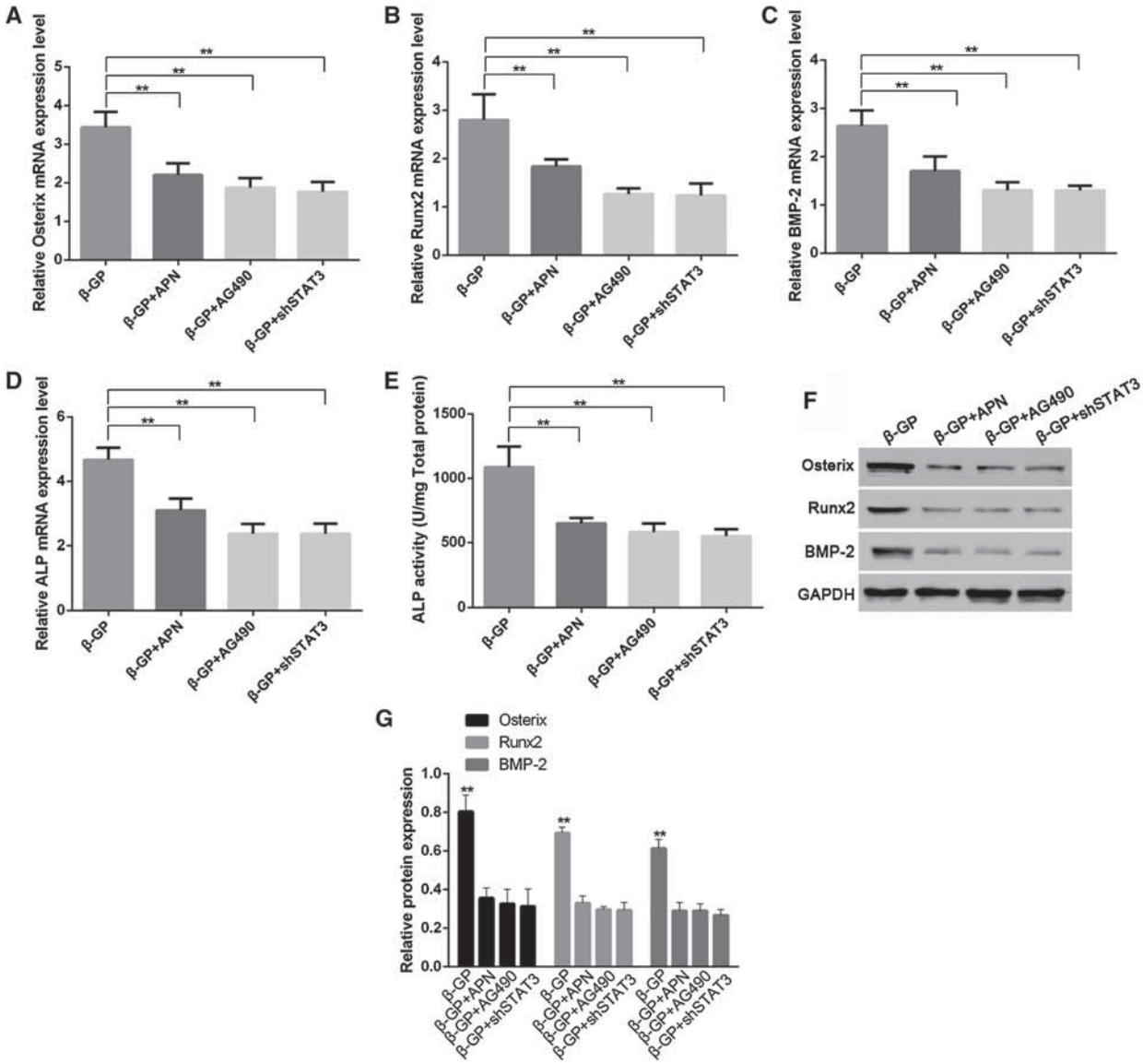


**Figure 6.** AG490 could also down regulate the expression of osterix, ALP, RUNX2 and BMP-2 in VSMCs treated with β-GP. (**A**) Relative osterix mRNA expression; (**B**) relative RUNX2 mRNA expression; (**C**) relative BMP-2 mRNA expression; (**D**) relative ALP mRNA expression; (**E**) effects of AG490 on ALP activity; (**F**) western blotting results of osterix, RUNX2 and BMP-2 protein expression and (**G**) gray value analysis of osterix, RUNX2 and BMP-2 protein expression.

transcription factor. In this study, we found that the expression levels of JAK2 and STAT3 did not change, however, β-GP could promote the expression of p-JAK2, p-STAT3 and osterix in VSMCs and APN could inhibit their up regulation (figure 4). β-GP could promote the transport of STAT3 into VSMCs, while APN could inhibit STAT3 transport into the nucleus (figure 5).

### 3.3 *JAK inhibitor AG490 could also down-regulate the expression of osterix and inhibit the osteogenic differentiation of VSMCs induced by β-GP*

We blocked the JAK2/STAT3 signaling pathway with the JAK inhibitor AG490, it was found that APN-like AG490 could also down-regulate the expression of osterix and inhibit the expression of ALP, RUNX2 and BMP-2 (figure 6).

## 4. Discussion

APN plays a protective role in myocardial ischemia through the APN/AdipoR1(APN receptor)/caveolin-3 pathway, this protective effect completely disappeared in diabetic patients with the impaired APN/AdipoR1/caveolin-3 pathway (Li *et al.* 2016). APN protects blood vessels, inhibits plaque and thrombosis by acting on the vascular system including endothelial cells, monocytes, macrophages, leukocytes, platelets and smooth muscle cells (Kawagoe *et al.* 2014). However, whether APN can inhibit vascular calcification has not been reported. In this study, we found that APN inhibited VSMC calcification in the cell model of VSMC calcification induced by β-GP. The inhibitory effect of APN was related to the JAK2/STAT3 signaling pathway.

JAK2 is a protein tyrosine kinase activated by a cytokine receptor. Activated JAK2 phosphorylates and activates cytoplasmic STAT3, then regulates the expression of genes related to cell survival, proliferation, cell cycle progression and angiogenesis, and participates in the growth and development of organisms and disease occurrence. In this study, we found that APN could inhibit osteogenic differentiation of VSMCs in β-GP-induced VSMC calcification. APN could inhibit the phosphorylation of STAT3 and prevent its translocation into the nucleus. When the JAK2 inhibitor AG490 was added, it could also inhibit the osteogenic differentiation of VSMCs induced by β-GP. These results suggested that APN inhibited VSMC calcification induced by β-GP through the JAK2/STAT3 signaling pathway.

STAT3 is an important transcription activator, and the nuclear localization of its phosphorylation could activate the transcription of a large number of downstream genes. It has been reported that STAT3 could bind to the promoter of osterix (Osx), a transcription factor associated with osteoblast differentiation and bone formation, and promotes the transcription of osterix and osteogenic differentiation (Huh and Lee 2013). In this study, we confirmed that both APN and JAK2 inhibitor AG490 could down-regulate osterix expression while inhibiting STAT3 phosphorylation into the nucleus. At the same time, the expression levels of molecular markers of VSMC osteogenic differentiation ALP, Runx2 and BMP-2 were significantly decreased.

## 5. Conclusions

In a word, this study indicated that APN protects VSMC from calcification induced by β-GP by inhibiting the JAK2/STAT3 signaling pathway and down-regulating the expression of the transcription factor osterix. APN may be one of the potential candidates for clinical treatment of vascular calcification. A further study on the protective mechanism of APN in cardiovascular diseases may provide new ideas for the treatment of cardiovascular diseases.

## Acknowledgements

This study was supported by the Beijing Lisheng Cardiovascular Health Foundation (LHJJ201611930) and Health and Family Planning Commission of Shanxi Province project (201601031).

## References

Cardenas V, Seo K, Sheth S and Meyr AJ 2018 Prevalence of lower-extremity arterial calcification in patients with diabetes mellitus complicated by foot disease at an urban US tertiary-care center. *J. Am. Podiatric. Med. Assoc.* **108** 267–271

Chen NX and Moe SM 2015 Pathophysiology of vascular calcification. *Curr. Osteoporos. Rep.* **13** 372–380

Chen SC, Huang JC, Su HM, Chiu YW, Chang JM, Hwang SJ and Chen HC 2018 Prognostic cardiovascular markers in chronic kidney disease. *Kidney Blood Pressure Res.* **43** 1363

Cheng HM, Wang JJ and Chen CH 2018 The role of vascular calcification in heart failure and cognitive decline. *Pulse (Basel)* **5** 144–153

Ding Y, Zhang D, Wang B, Zhang Y, Wang L, Chen X, Li M, Tang Z and Wang C 2016 APPL1-mediated activation of STAT3 contributes to inhibitory effect of adiponectin on hepatic gluconeogenesis. *Mol. Cell. Endocrinol.* **433** 12–19

Guo R, Han M, Song J, Liu J and Sun Y 2018 Adiponectin and its receptors are involved in hypertensive vascular injury. *Mol. Med. Rep.* **17** 209–215

Huh JE and Lee SY 2013 IL-6 is produced by adipose-derived stromal cells and promotes osteogenesis. *Biochim. Biophys. Acta* **1833** 2608–2616

Jasani R, Hase N, Kumar R, Dedhia P, Jamale T and Bajpai D 2018 Predictors of coronary calcification in Indian hemodialysis patients. *Saudi J. Kidney Dis. Transpl.* **29** 822–827

Kawagoe J, Ishikawa T, Iwakiri H, Date H, Imamura T and Kitamura K 2014 Association between adiponectin production in coronary circulation and future cardiovascular events in patients with coronary artery disease. *Int. Heart J.* **55** 239–243

Leopold JA 2015 Vascular calcification: Mechanisms of vascular smooth muscle cell calcification. *Trends Cardiovasc. Med.* **25** 267–274

Li H, Yao W, Liu Z, Xu A, Huang Y, Ma XL, Irwin MG and Xia Z 2016 Hyperglycemia abrogates ischemic postconditioning cardioprotection by impairing AdipoR1/Caveolin-3/STAT3 signaling in diabetic rats. *Diabetes* **65** 942–955

Liu Y, Sen S, Wannaiampikul S, Palanivel R, Hoo RL, Isserlin R, Bader GD, Tungtrongchitr R, Deshaies Y, Xu A and Sweeney G 2015 Metabolomic profiling in liver of adiponectin-knockout mice uncovers lysophospholipid metabolism as an important target of adiponectin action. *Biochem. J.* **469** 71–82

Moon HS and Mantzoros CS 2013 Adiponectin and metformin additively attenuate IL1beta-induced malignant potential of colon cancer. *Endocr.-Relat. Cancer* **20** 849–859

Nitta K and Ogawa T 2015 Vascular calcification in end-stage renal disease patients. *Contrib. Nephrol.* **185** 156–167

Pajvani UB, Du X, Combs TP, Berg AH, Rajala MW, Schulthess T, Engel J, Brownlee M and Scherer PE 2003 Structure function studies of the adipocyte-secreted hormone Acrp30/adiponectin: Implications for metabolic regulation and bioactivity. *J. Biol. Chem.* **278** 9073–9085

Sun H, Zhang Y, Gao P, Li Q, Sun Y, Zhang J and Xu C 2011 Adiponectin reduces C-reactive protein expression and downregulates STAT3 phosphorylation induced by IL-6 in HepG2 cells. *Mol. Cell. Biochem.* **347** 183–189

Uemura Y, Shibata R, Ohashi K, Enomoto T, Kambara T, Yamamoto T, Ogura Y, Yuasa D, Joki Y, Matsuo K, Miyabe M, Kataoka Y, Murohara T and Ouchi N 2013 Adipose-derived factor CTRP9 attenuates vascular smooth muscle cell proliferation and neointimal formation. *FASEB J.* **27** 25–33

Wang H, Zhang H, Zhang Z, Huang B, Cheng X, Wang D, La Gahu Z, Xue Z, Da Y, Li D, Yao Z, Gao F, Xu A and Zhang R 2016 Adiponectin-derived active peptide ADP355 exerts antiinflammatory and anti-fibrotic activities in thioacetamideinduced liver injury. *Sci. Rep.* **6** 19445

Zhang C, Liao Y, Li Q, Chen M, Zhao Q, Deng R, Wu C, Yang A, Guo Z, Wang D and He X 2013 Recombinant adiponectin ameliorates liver ischemia reperfusion injury via activating the AMPK/eNOS pathway. *PLoS ONE* **8** e66382

Zhang R, Yin X, Shi H, Wu J, Shakya P, Liu D and Zhang J 2014 Adiponectin modulates DCA-induced inflammation via the ROS/NF-κ B signaling pathway in esophageal adenocarcinoma cells. *Dig. Dis. Sci.* **59** 89–97

Corresponding editor: BJ Rao